

# ANALYSIS OF TWO-SCALE FINITE VOLUME ELEMENT METHOD FOR ELLIPTIC PROBLEM

VICTOR E. GINTING

ABSTRACT. In this paper we propose and analyze a class of finite volume element method for solving a second order elliptic boundary value problem whose solution is defined in more than one length scales. The method has the ability to incorporate the small scale behaviors of the solution on the large scale one. This is achieved through the construction of the basis functions on each element that satisfy the homogeneous elliptic differential equation. Furthermore, the method enjoys numerical conservation feature which is highly desirable in many applications. Existing analyses on its finite element counterpart reveal that there exists a resonance error between the mesh size and the small length scale. This result motivates an oversampling technique to overcome this drawback. We develop an analysis of the proposed method under the assumption that the coefficients are of two scales and periodic in the small scale. The theoretical results are confirmed experimentally by several convergence tests. Moreover, we present an application of the method to flows in porous media.

## 1. INTRODUCTION

Understanding and quantification of the phenomena and processes arising in engineering and physics often involve solving boundary value problems with many scales. The existence of heterogeneities, such as in the flow in porous media formations for example, occurs either globally or locally which influence the behavior of the phenomena under investigation. Consequently, attempts to primitively solve these problems numerically are challenging since a vast amount degree of freedoms have to be devoted in order to produce the most accurate predictions.

Besides utilizing the parallel computing technology which does not actually reduce the problem size, there have been significant efforts to develop methods of obtaining effective parameters that are defined on coarser models. This is also in conjunction with engineering work that often requires only the knowledge of the processes on the large scale. The common terminology for this practice is upscaling. Among the many literatures that deal with these issues are [5, 7, 8, 11, 20] and references cited therein. In general, the more simplified mathematical descriptions were motivated by homogenization theory (see, e.g. [18]).

A somewhat new direction in tackling this problem has been developed recently (cf. e.g. [1, 9, 15, 16]). The numerical methods presented in these papers have the ability to capture the small scales effect on the large scale solution without resolving the small scale details. In [15, 16] for example, this is implemented by devising the so called oscillatory basis functions which are incorporated into the finite element formulation on the coarse grid,

hence the name multiscale finite element method. The basis functions serve as the building block of all small scale structures inherited from the original problem, so that they are set to satisfy the leading order homogeneous elliptic equation in each coarse element. It should be noted that the effectiveness of the multiscale finite element method is more significant when the coarse element size is substantially larger than the small scale length.

The analyses and convergence tests for the case of two-scale periodic coefficients reported in [15, 16] reveal that there exists an interaction between the coarse element size and the small scale length. This kind of error, referred to as resonance error, is the ratio of these two numbers. In effect, the error becomes large when these two numbers are close to each other. This brings the use of oversampling strategy reported in [10]. Since it is believed that the resonance error is originated from the boundary layer in the first order corrector of the local solution, then solving the basis functions on larger domain than the specified coarse element would diminish the boundary layer. This is the meaning of oversampling. One drawback of the oversampling technique is that the resulting solution is nonconforming. However, for some practical purposes where the sought quantity is the gradient of the solution (flux) nonconformity should not cause a serious harm. The errors associated with this nonconformity have been studied in [10, 21]. In particular, the authors of [21] have shown that by a careful choice of global formulation of the problem, one can reduce the nonconforming error.

In addition to capturing small scale effects on the large one, many engineering and physical applications such as those arising in the petroleum reservoir simulations, groundwater hydrology and environmental remediation, desire to develop numerical methods that have certain conservation features. This may be achieved by using mixed finite element, discontinuous Galerkin finite element, and finite volume methods. The finite volume method (box schemes) has the simplicity of the finite difference method [13], and at the same time enjoys the flexibility of the finite element method. For this reason this method is referred to as finite volume element method [12, 19]. Recently, the trend is to view the finite volume element method as a perturbation of finite element method using certain interpolation operator. This way, analysis of the method uses substantially the existing finite element results and techniques [2, 3, 4].

In this paper we propose a two-scale finite volume element method for solving a class of second order elliptic boundary value problems. We will follow the ideas from [10, 16, 15] for the construction of the basis functions. An oversampling strategy will be utilized to produce the nonconforming basis functions. The difference is the variational formulation will be defined through finite volume method. Similar procedure has been implemented in [17]. For the analysis, we concentrate on the two-scale periodic coefficients, so that we may use the technique of the homogenization theory to obtain asymptotic expansion of the solution. The main result is based on estimating the perturbation of this two-scale finite volume element method with respect to its finite element counterpart.

The paper is organized as follows. In section 2 we present the model problem and revisit several existing notations and tools required for developing the two-scale finite volume element method and its analysis. Then section 3 is devoted to presenting the formulation of two-scale finite volume element method. It includes an overview of homogenization theory

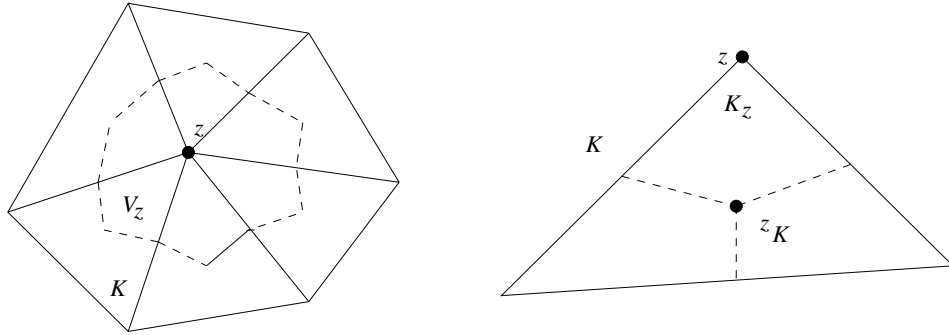


FIGURE 1. *Left:* Portion of triangulation sharing a common vertex  $z$  and its control volume. *Right:* Partition of a triangle  $K$  into three quadrilaterals

that will be used in the construction of the oversampling method and also in the subsequent analysis. The method is focused on a two-dimensional space problems. However, extension of the method to three-dimensional problems is straightforward. In section 4 we give an  $H^1$  estimate of the error, which will be for the case when the mesh size is larger than the fluctuating scale of the continuous problem. Numerical examples aimed to investigate the convergence and accuracy of the method are given in section 5 on problems with periodic and random coefficients. Section 6 is reserved for concluding remarks.

## 2. MODEL PROBLEM AND PRELIMINARIES

We seek the solution  $u_\epsilon = u(x, x/\epsilon)$  of the following boundary value problem:

$$(2.1) \quad \begin{aligned} L_\epsilon u_\epsilon &\equiv -\nabla \cdot (A(x/\epsilon)\nabla u_\epsilon) = f(x) && \text{in } \Omega \subset \mathbb{R}^2, \\ u_\epsilon &= 0 && \text{on } \partial\Omega, \end{aligned}$$

where  $\Omega \subset \mathbb{R}^2$  is a bounded polygonal domain,  $\epsilon > 0$  is a small parameter, and  $A(x/\epsilon) = (A_{ij}(x/\epsilon))$  is a  $2 \times 2$  symmetric positive definite matrix, i.e., there exists constants  $\beta > \alpha > 0$  such that  $\alpha|\xi|^2 \leq \xi^t A \xi \leq \beta|\xi|^2$  for any vector  $\xi \in \mathbb{R}^2$  and for almost every  $x \in \Omega$ . Furthermore, we assume that the coefficients  $A_{ij}(y)$  is sufficiently smooth periodic functions (with period 1) in  $y$  in a unit square  $Y = [0, 1] \times [0, 1]$ . In our analysis it suffices to assume that  $A_{ij}(y) \in W_p^2(Y)$  ( $p > 2$ ).

In what follows we describe some preliminaries that are necessary for the description of our numerical method and its analysis. Let  $\{T_h\}_{0 < h < 1}$  be a family of quasiuniform triangulations of a bounded polygonal domain  $\Omega$ , with  $h_K$  denotes the diameter of the triangle  $K \in T_h$ , and  $h = \max_K \{h_K\}$ . Given the triangulation  $T_h$  we describe the construction of the control volumes as follows. Consider a triangle  $K$ , and let  $z_K$  be its barycenter. The triangle  $K$  is divided into three quadrilaterals of equal area by connecting  $z_K$  to the midpoints of its three edges. We denote these quadrilaterals by  $K_z$ , where  $z \in Z_h(K)$ , are the vertices of  $K$ . Also we denote  $Z_h = \bigcup_K Z_h(K)$ , and  $Z_h^0 =$  interior vertices of  $Z_h$ . The control volume  $V_z$  is defined as the union of the quadrilaterals  $K_z$  sharing the vertex  $z$  (see Figure 1). Let  $K$  be a domain in  $\mathbb{R}^2$ . We denote by  $L_2(K)$ , the space of square inte-

grable real functions over  $K$ ,  $(\cdot, \cdot)_K$  the inner product in  $L_2(K)$ ,  $\|\cdot\|_{H^m(K)}$  and  $|\cdot|_{H^m(K)}$ , the norm and seminorm of the Sobolev space  $H^m(K)$  for  $m \in \mathbb{N}$ . We also introduce the “broken” norm  $\|\cdot\|_{m,h}$  such that  $\|v\|_{m,h} = \{\sum_{K \in T_h} \|v\|_{H^m(K)}^2\}^{1/2}$ , and its corresponding seminorm  $|\cdot|_{m,h}$  such that  $|v|_{m,h} = \{\sum_{K \in T_h} |v|_{H^m(K)}^2\}^{1/2}$ . Also we denote by  $\|\cdot\|_{W_p^m(K)}$  and  $|\cdot|_{W_p^m(K)}$ , respectively the norm and seminorm of the Sobolev space  $W_p^m(K)$ ,  $m \in \mathbb{N}$ ,  $p \geq 1$ . Finally we designate by  $\langle \cdot \rangle_K$  the mean of a function over  $K$ . We note that we suppress the  $K$  in the notations whenever  $K = \Omega$ , and suppress the index  $m$  whenever  $m = 0$ , i.e.,  $H^0(K) = L_2(K)$ . Throughout the paper,  $C$  and  $c$  (sometimes with indices) will denote a generic constant independent of  $h$  and  $\epsilon$ .

We denote the following two finite dimensional spaces:

$$(2.2) \quad X_h = \{\chi \in H_0^1(\Omega) : \chi|_K \text{ is linear, } \chi|_{\partial\Omega} = 0\},$$

$$(2.3) \quad Y_h = \{\xi \in L_2(\Omega) : \xi|_{V_z} \text{ is constant, } z \in Z_h^0, \xi|_{V_z} = 0 \text{ if } z \in \partial\Omega\}.$$

In the sections that follow we use the following interpolation operator  $I_h : X_h \rightarrow Y_h$  such that  $\forall \chi \in X_h$

$$(2.4) \quad I_h \chi = \sum_{z \in Z_h^0} \chi(z) \Psi_z,$$

where  $\Psi_z$  is the characteristic function of the control volume  $V_z$ . Below we list several properties of  $I_h$  (see [2, 4] for details):

$$(2.5) \quad (\chi, I_h \phi) = (\phi, I_h \chi), \quad \forall \chi, \phi \in X_h,$$

$$(2.6) \quad c_1 \|\chi\|^2 \leq |||\chi|||^2 \leq c_2 \|\chi\|^2, \quad \forall \chi \in X_h, \quad c_2 > c_1 > 0, \quad |||\chi|||^2 = (\chi, I_h \chi),$$

$$(2.7) \quad \int_K I_h \chi \, dx = \int_K \chi \, dx, \quad \forall \chi \in X_h, \quad \text{for any } K \in T_h,$$

$$(2.8) \quad \int_e I_h \chi \, ds = \int_e \chi \, ds, \quad \forall \chi \in X_h, \quad \text{for any side } e \text{ of } K \in T_h,$$

$$(2.9) \quad \|I_h \chi\|_{L_\infty(e)} \leq \|\chi\|_{L_\infty(e)}, \quad \forall \chi \in X_h, \quad \text{for any side } e \text{ of } K \in T_h,$$

$$(2.10) \quad \|\chi - I_h \chi\|_{L_p(K)} \leq Ch_K |\chi|_{W_p^1(K)}, \quad \forall \chi \in X_h, \quad 1 \leq p < \infty.$$

### 3. A TWO-SCALE FINITE VOLUME ELEMENT METHOD WITH OVERSAMPLING

This section is devoted to the formulation of two-scale finite volume element method for solving (2.1) and its necessary venue for the analysis. In subsection 3.1 we briefly review a homogenization theory that will be needed for this purpose. The detail of oversampling is presented in subsection 3.2. Then the formulation of the finite volume element method is elaborated in subsection 3.3. In the following, the Einstein summation is assumed wherever it applies.

**3.1. Overview of homogenization theory.** Here we review some results from homogenization theory. First we define  $N_k(y)$ ,  $k = 1, 2$  to be the periodic solution in the unit square  $Y$  with  $\langle N_k \rangle_Y = 0$  that satisfies the equation

$$(3.1) \quad \nabla^y \cdot (A(y) \nabla^y N_k(y)) = -\nabla_i^y A_{ik}(y).$$

Here  $\nabla^y$  is the gradient with respect to the variable  $y$  and  $\nabla_i^y$  is the  $i$ -th component of the  $\nabla^y$ . By homogenization theory (cf. [18]), the solution of (2.1) can be expanded as

$$(3.2) \quad u_\epsilon = u_0 + \epsilon N_k(x/\epsilon) \nabla_k u_0 + \epsilon \theta^u,$$

where  $\nabla_k$  is the  $k$ -th component of  $\nabla$ . The function  $u_0$  is the solution of the following homogenized boundary value problem:

$$(3.3) \quad \begin{aligned} -\nabla \cdot (A^* \nabla u_0) &= f & \text{in } \Omega, \\ u_0 &= 0 & \text{on } \partial\Omega, \end{aligned}$$

where the entries of  $A^*$ , denoted by  $A_{ij}^*$ , is expressed as

$$(3.4) \quad A_{ij}^* = \int_Y A_{ik} (\delta_{kj} + \nabla_k^y N_j) dy.$$

Regarding  $\theta^u$ , we have the following estimate [18]:

**Lemma 3.1.** *Let  $\theta^u$  be the corrector in (3.2). Then there exists a constant  $C > 0$  independent of  $\epsilon$  such that*

$$(3.5) \quad \epsilon |\theta^u|_1 \leq C \sqrt{\epsilon}.$$

**3.2. Oversampling and construction of the solution space.** In this subsection we present the oversampling strategy that will be combined with the finite volume element method. We construct an intermediate basis functions  $\{\psi_\epsilon^i, i = 1, 2, 3\}$  in an oversampled triangle domain  $S \supset K$ ,  $\text{diam}(S) > 2h_K$  by solving

$$(3.6) \quad L_\epsilon \psi_\epsilon^i = -\nabla \cdot (A(x/\epsilon) \nabla \psi_\epsilon^i) = 0 \quad \text{in } S,$$

where  $\psi_\epsilon^i$  is piecewise linear along  $\partial S$ , and  $\psi_\epsilon^i(s_j) = \delta_{ij}$ , with  $s_j, j = 1, 2, 3$  being the vertices of  $S$  (see Figure 2). It follows from this construction that  $\psi_\epsilon^i$  exhibit similar structure to  $u_\epsilon$ . To be specific,  $\psi_\epsilon^i$  has the following asymptotic expansion:

$$(3.7) \quad \psi_\epsilon^i = \psi_0^i + \epsilon N_k(x/\epsilon) \nabla_k \psi_0^i + \epsilon \theta^i,$$

where  $\psi_0^i$  is the linear homogenized part of  $\psi_\epsilon^i$ . Furthermore, we may write  $\theta^i = \eta_k \nabla_k \psi_0^i$ , where  $\eta_k, k = 1, 2$ , satisfy the following problem:

$$(3.8) \quad \begin{aligned} \nabla \cdot (A(x/\epsilon) \nabla \eta_k) &= 0 & \text{in } S \\ \eta_k &= N_k & \text{on } \partial S. \end{aligned}$$

The function  $\eta_k$  enjoys the following property [10]:

**Lemma 3.2.** *Let  $K \in T_h$  such that  $K \subset S$ . There exists a constant  $C > 0$  independent of  $\epsilon$  and  $h_K$  such that*

$$(3.9) \quad \|\nabla \eta_k\|_{L^\infty(K)} \leq \frac{C}{h_K}.$$

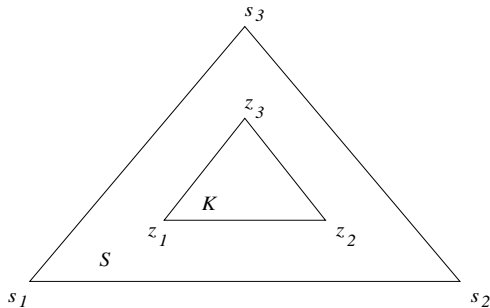


FIGURE 2. Oversampling of basis functions on a substantially larger domain than triangle  $K$ .

Next, the basis functions  $\{\phi_\epsilon^i, i = 1, 2, 3\}$  on  $K$  are constructed by linear combination of  $\{\psi_\epsilon^i, i = 1, 2, 3\}$ :

$$(3.10) \quad \phi_\epsilon^i = \sum_{j=1}^3 c_{ij} \psi_\epsilon^j.$$

Substituting (3.7) to (3.10), we see that  $\phi_\epsilon^i$  can be expanded as follows:

$$(3.11) \quad \phi_\epsilon^i = \phi_0^i + \epsilon N_k(x/\epsilon) \nabla_k \phi_0^i + \epsilon c_{ij} \theta^j,$$

where

$$(3.12) \quad \phi_0^i = \sum_{j=1}^3 c_{ij} \psi_0^j.$$

The constants  $c_{ij}$  are obtained by setting  $\phi_0^i(z_j) = \delta_{ij}$  which gives a system of linear equation. It is straightforward to see that the  $3 \times 3$  matrix in this linear system is invertible. Furthermore, since the oversampled domain  $S$  is not extremely larger than the triangle  $K$ , the matrix is well conditioned. Now we denote the space of the approximate solution by  $V_h$ , which is defined as the space spanned by  $\phi_\epsilon^i|_K$ . We note that by this construction, the basis functions are not continuous across  $\partial K$ . We also set the basis functions to be zero on  $\partial\Omega$ . Consequently  $V_h$  is no longer a subset of  $H^1(\Omega)$ .

Now we have the tool to expand the functions that belong to the space of our approximate solution  $V_h$ . So consider  $v_\epsilon^h \in V_h$ . Since the expansion of the basis functions was conducted on a triangle  $K$ , we will also have the asymptotic expansion for  $v_\epsilon^h$  on  $K$ . First we write  $v_0^h = v_0^h(z_i) \phi_0^i$ ,  $z_i \in Z_h(K)$ . Moreover, since  $\theta^j = \eta_k \nabla_k \psi_0^j$  we may define  $\theta^h$  using the following equivalent representations:

$$(3.13) \quad \theta^h = v_0^h(z_i) c_{ij} \theta^j = v_0^h(z_i) c_{ij} \eta_k \nabla_k \psi_0^j = v_0^h(z_i) \eta_k \nabla_k \phi_0^i = \eta_k \nabla_k v_0^h.$$

Then by setting  $v_\epsilon^h = v_0^h(z_i) \phi_\epsilon^i$  for  $z_i \in Z(K)$ , and using (3.11) and (3.13), we have the following asymptotic expansion for  $v_\epsilon^h \in V_h$ :

$$(3.14) \quad v_\epsilon^h = v_0^h + \epsilon N_k(x/\epsilon) \nabla_k v_0^h + \epsilon \theta^h$$

on each triangle  $K \in T_h$ .

**3.3. Formulation of the method.** At this point, we are in a position to describe the two-scale finite volume element method for (2.1) that incorporates the small scale features: to seek  $u_\epsilon^h \in V_h$  that satisfies the following local conservation property:

$$(3.15) \quad - \int_{\partial V_z} (A(x/\epsilon) \nabla u_\epsilon^h) \cdot \vec{n} \, ds = \int_{V_z} f \, dx, \quad \forall z \in Z_h^0,$$

where  $\vec{n}$  is the unit normal vector pointing outward on  $\partial V_z$ . Obviously, this construction requires that the number of control volumes  $V_z$  be equal to the dimension of  $V_h$ . We note that this formulation may be equivalently written as the following variational problem: Find  $u_\epsilon^h \in V_h$  such that

$$(3.16) \quad a_{FV}(u_\epsilon^h, \chi) = \sum_{z \in Z_h^0} \chi(z) \int_{V_z} f \, dx \quad \forall \chi \in X_h,$$

where the form  $a_{FV}(\cdot, \cdot) : \tilde{H}_h^2 \times H_h^2 \rightarrow \mathbb{R}$  is defined by

$$(3.17) \quad a_{FV}(v, \chi) = - \sum_{z \in Z_h^0} \chi(z) \int_{\partial V_z} (A(x/\epsilon) \nabla v) \cdot \vec{n} \, ds,$$

with  $\tilde{H}_h^2 = H^2(\Omega) + V_h$  and  $H_h^2 = H^2(\Omega) + X_h$ . In [2] it has been shown that using the interpolation operator  $I_h$  in (2.4), we have

$$(3.18) \quad \sum_{z \in Z_h^0} \chi(z) \int_{V_z} f \, dx = (f, I_h \chi).$$

Now we can give another equivalent representation of  $a_{FV}(v, \chi)$ . Consider a triangle  $K$  and a control volume  $V_z$  such that  $K \cap V_z \neq \emptyset$ . Then using Green's formula we get

$$(3.19) \quad \int_{K \cap V_z} L_\epsilon v \, dx = - \int_{\partial K \cap V_z} (A(x/\epsilon) \nabla v) \cdot \vec{n} \, ds - \int_{\partial V_z \cap K} (A(x/\epsilon) \nabla v) \cdot \vec{n} \, ds.$$

This equality and the interpolation operator  $I_h$  allows us to get

$$(3.20) \quad \begin{aligned} a_{FV}(v, \chi) &= - \sum_{K \in T_h} \sum_{z \in Z_h(K)} \int_{\partial V_z \cap K} (A(x/\epsilon) \nabla v) \cdot \vec{n} \, I_h \chi \, ds \\ &= \sum_{K \in T_h} \left\{ (L_\epsilon v, I_h \chi)_K + ((A(x/\epsilon) \nabla v) \cdot \vec{n}, I_h \chi)_{\partial K} \right\}. \end{aligned}$$

By combining all these identities we may write the following equivalent Petrov-Galerkin formulation of the *two-scale finite volume element* problem: Find  $u_\epsilon^h \in V_h$  such that

$$(3.21) \quad a_{FV}(u_\epsilon^h, \chi) = (f, I_h \chi) \quad \forall \chi \in X_h,$$

with  $a_{FV}(\cdot, \cdot)$  as in (3.20).

In the standard finite volume element method, there is well developed technique for the error analysis based on the existing results from its standard finite element counterpart (see [2, 4] for detail investigation). The main idea is in viewing the finite volume element as a

perturbation of finite element method with the help of the interpolation operator  $I_h$ . This way, one can tap into existing analysis in the Galerkin finite element method to derive the error estimates for finite volume element method.

In this paper we will follow similar procedure. However, due to the specific construction of the basis functions and the corresponding finite dimensional space of the approximate solution  $V_h$ , that accounts for the scale features, we will employ Petrov-Galerkin formulation. First, we introduce the Petrov-Galerkin formulation of the *two-scale finite element* problem associated with (2.1): Find  $\tilde{u}_\epsilon^h \in V_h$  such that

$$(3.22) \quad a_{FE}(\tilde{u}_\epsilon^h, \chi) = (f, \chi) \quad \forall \chi \in X_h,$$

where

$$(3.23) \quad a_{FE}(v_\epsilon^h, \chi) = \sum_{K \in T_h} (A(x/\epsilon) \nabla v_\epsilon^h, \nabla \chi)_K, \quad \forall v_\epsilon^h \in V_h, \chi \in X_h.$$

By Green's formula we may write  $a_{FE}(\cdot, \cdot)$  as

$$(3.24) \quad a_{FE}(v_\epsilon^h, \chi) = \sum_{K \in T_h} \left\{ (L_\epsilon v_\epsilon^h, \chi)_K + (A(x/\epsilon) \nabla v_\epsilon^h \cdot \vec{n}, \chi)_{\partial K} \right\}, \quad \forall v_\epsilon^h \in V_h, \chi \in X_h.$$

Moreover, by the construction of the basis functions of  $V_h$  we have

$$(3.25) \quad (L_\epsilon v_\epsilon^h, I_h \chi)_K = (L_\epsilon v_\epsilon^h, \chi)_K = 0, \quad \forall v_\epsilon^h \in V_h, \chi \in X_h.$$

Using (3.24) and (3.20), we may define the following bilinear form  $D : V_h \times X_h \rightarrow \mathbb{R}$ :

$$(3.26) \quad \begin{aligned} D(v_\epsilon^h, \chi) &= a_{FE}(v_\epsilon^h, \chi) - a_{FV}(v_\epsilon^h, I_h \chi) \\ &= \sum_{K \in T_h} ((A(x/\epsilon) \nabla v_\epsilon^h) \cdot \vec{n}, \chi - I_h \chi)_{\partial K} \end{aligned}$$

This bilinear form characterizes the two-scale finite volume element method as the perturbation of two-scale finite element method. Our aim now is to estimate (3.26), and in turn use the existing results of the two-scale finite element method to obtain the convergence of the two-scale finite volume element method.

#### 4. CONVERGENCE ANALYSIS OF THE METHOD FOR CASE $\epsilon \ll h$

As mentioned earlier, the analysis proceeds with quantification of the perturbation between the two-scale finite volume element method and its finite element counterpart. In this section we estimate (3.26), show the inf-sup condition of the bilinear form guaranteeing the existence and uniqueness of the solution, and prove the error estimate. First we establish the following lemma that will be used in the subsequent proof. We define a  $2 \times 2$  matrix  $B(x/\epsilon)$  such that its entries are written as

$$(4.1) \quad B_{ij} = A_{ij} + \epsilon A_{ik} \nabla_k N_j,$$

where  $N_j$  is as in subsection 3.1.



**Lemma 4.1.** *Assume that there exists  $c_2 > c_1 > 0$  such that*

$$(4.2) \quad c_1 |\xi|^2 \leq \xi_i B_{ij} \xi_j \leq c_2 |\xi|^2 \quad \forall \xi \in \mathbb{R}^2.$$

*Then there exists  $C_2 > C_1 > 0$  such that*

$$(4.3) \quad C_1 |\nabla v_\epsilon^h|_K \leq |\nabla v_0^h|_K \leq C_2 |\nabla v_\epsilon^h|_K$$

*for every  $v_\epsilon^h \in V_h$  and for each  $K \in T_h$ .*

*Proof.* In what follows all the estimates are taken over the triangle  $K$ . Using (3.14) and (3.13) and noting that  $v_0^h$  is linear in  $K$ , we have the following equality:

$$(4.4) \quad \begin{aligned} A_{ij} \nabla_j v_\epsilon^h &= A_{ij} \nabla_j v_0^h + A_{ij} \nabla_j \left( \epsilon N_k \nabla_k v_0^h \right) + \epsilon A_{ij} \nabla_j \theta^h \\ &= (A_{ij} + \epsilon A_{ik} \nabla_k N_j + \epsilon A_{ik} \nabla_k \eta_j) \nabla_j v_0^h \\ &= (B_{ij} + \epsilon A_{ik} \nabla_k \eta_j) \nabla_j v_0^h. \end{aligned}$$

Multiplying (4.4) by  $\nabla_i v_0^h$  we have

$$(4.5) \quad \nabla_i v_0^h A_{ij} \nabla_j v_\epsilon^h = \nabla_i v_0^h (B_{ij} + \epsilon A_{ik} \nabla_k \eta_j) \nabla_j v_0^h.$$

Now by Lemma 3.2 we may use the assumption (4.2) to the term  $B_{ij} + \epsilon A_{ik} \nabla_k \eta_j$ , so that

$$(4.6) \quad \beta |\nabla v_0^h| |\nabla v_\epsilon^h| \geq \nabla_i v_0^h A_{ij} \nabla_j v_\epsilon^h = \nabla_i v_0^h (B_{ij} + \epsilon A_{ik} \nabla_k \eta_j) \nabla_j v_0^h \geq c_1 |\nabla v_0^h|^2,$$

from which we obtain the right hand side inequality of (4.3). Similarly, multiplying (4.4) by  $\nabla_i v_\epsilon^h$ , and by positive definiteness of  $A$ , we obtain the result for the left hand side of (4.3).  $\square$

**4.1. Estimate on the functional  $D$ .** In this subsection we estimate the functional defined in (3.26). By substituting (3.14) in (3.26) and noting that  $v_0^h$  in (3.14) is piecewise linear, we may rewrite (3.26) in the form

$$(4.7) \quad \begin{aligned} D(v_\epsilon^h, \chi) &= \sum_{K \in T_h} \left( (B(x/\epsilon) \nabla v_0^h) \cdot \vec{n}, \chi - I_h \chi \right)_{\partial K} \\ &\quad + \sum_{K \in T_h} \left( (A(x/\epsilon) \epsilon \nabla \theta^h) \cdot \vec{n}, \chi - I_h \chi \right)_{\partial K} \end{aligned}$$

for any  $\chi \in X_h$  where the entries of  $B$  are as in (4.1). The following two lemmas are devoted to estimate the two terms in (4.7).

**Lemma 4.2.** *Assume that the coefficient matrix  $A(y)$  is 1-periodic functions along each edge  $e$  of a triangle  $K$ . Then for every  $\chi \in X_h$  there exists constant  $C > 0$  independent of  $\epsilon$  and  $h$  such that*

$$(4.8) \quad \int_e (B(x/\epsilon) \nabla v_0^h) \cdot \vec{n} (\chi - I_h \chi) ds \leq C \frac{\epsilon}{h} |v_\epsilon^h|_{H^1(K)} |\chi|_{H^1(K)}$$

*for every edge  $e$  of a triangle  $K$ .*

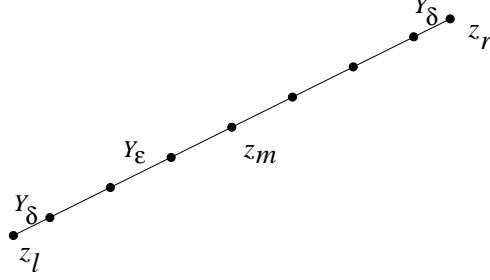


FIGURE 3. Partition of an edge  $e$  into sub-segments  $Y_\epsilon$  of size  $\epsilon$  and possibly two segments  $Y_\delta$  of size less than  $\epsilon$ .

*Proof.* Since the matrix  $A$  is 1-periodic along the edge, so is the matrix  $B$  defined by (4.1). Choose a constant matrix  $\tilde{B}$  whose entries will be determined later. Since  $\nabla v_0^h \cdot \vec{n}$  is constant on  $e$ , by (2.8) we have

$$(4.9) \quad \int_e (B(x/\epsilon) \nabla v_0^h) \cdot \vec{n} (\chi - I_h \chi) ds = \int_e ((B(x/\epsilon) - \tilde{B}) \nabla v_0^h) \cdot \vec{n} (\chi - I_h \chi) ds \\ = n_i \nabla_j v_0^h \int_e (B_{ij}(x/\epsilon) - \tilde{B}_{ij}) (\chi - I_h \chi) ds,$$

where we have used Einstein's summation on the last line. We note that  $I_h \chi$  is discontinuous along the edge  $e$ . Let  $z_l$  and  $z_r$  be the two vertices connected by edge  $e$ , and  $z_m$  be the point of discontinuity (which is the midpoint  $e$ ), and thus the integration in (4.9) may be broken up into integration along  $(z_l, z_m)$  plus integration along  $(z_m, z_r)$ . Starting from  $z_m$  we may break up the segment  $(z_l, z_m)$  into a number of sub-segments  $Y_\epsilon$  each of which has size  $\epsilon$  and possibly one sub-segment  $Y_\delta$  of size  $\delta < \epsilon$  (see Figure 3). Similar partition may be implemented for segment  $(z_m, z_r)$ . This partition implies that the integration in (4.9) may be broken up into the sum of integral over all the sub-segments. Now it is obvious that the matrix  $B$  is periodic with respect to the sub-segment  $Y_\epsilon$ . In what follows we will estimate the integral (4.9) over the sub-segments  $Y_\epsilon$  and  $Y_\delta$ . We choose the matrix  $\tilde{B}$  to have the following entries:

$$(4.10) \quad \tilde{B}_{ij} = \frac{1}{|Y_\epsilon|} \int_{Y_\epsilon} B_{ij} ds$$

Obviously the estimate for integral over  $Y_\delta$  is straightforward, since we have  $|B_{ij} - \tilde{B}_{ij}|$  bounded, and  $|\chi - I_h \chi| \leq C |\nabla \chi| \epsilon$  in  $Y_\delta$ . Hence,

$$(4.11) \quad \int_{Y_\delta} (B_{ij} - \tilde{B}_{ij}) (\chi - I_h \chi) ds \leq C \frac{\epsilon^2}{h} |\chi|_{H^1(K)},$$

where we have used the inverse inequality for  $\chi$ . Moreover, by choosing  $\tilde{B}$  as in (4.10), we have the following identity:

$$(4.12) \quad \int_{Y_\epsilon} (B_{ij} - \tilde{B}_{ij}) (\chi - I_h \chi) ds = \int_{Y_\epsilon} (B_{ij} - \tilde{B}_{ij}) \chi ds = \int_{Y_\epsilon} (B_{ij} - \tilde{B}_{ij}) (\chi - \tilde{\chi}) ds,$$

where

$$(4.13) \quad \tilde{\chi} = \frac{1}{|Y_\epsilon|} \int_{Y_\epsilon} \chi \, ds$$

Consequently, Poincare-Friedrich inequality and scaling argument gives us

$$(4.14) \quad \|B_{ij} - \widetilde{B}_{ij}\|_{L_2(Y_\epsilon)} \leq C \sqrt{\epsilon} \|\nabla^y B_{ij}\|_{L_2(0,1)} \leq C \sqrt{\epsilon}.$$

Furthermore, due to the fact that  $\chi$  is linear on the edge  $e$ , we also have

$$(4.15) \quad \|\chi - \tilde{\chi}\|_{L_2(Y_\epsilon)} \leq C \epsilon^{3/2} |\nabla \chi|.$$

Hence, using (4.12), Cauchy-Schwarz inequality, (4.14), and (4.15) we have the following estimate:

$$(4.16) \quad \begin{aligned} \int_{Y_\epsilon} (B_{ij} - \widetilde{B}_{ij}) (\chi - I_h \chi) \, ds &\leq \|B_{ij} - \widetilde{B}_{ij}\|_{L_2(Y_\epsilon)} \|\chi - \tilde{\chi}\|_{L_2(Y_\epsilon)} \\ &\leq C \epsilon^2 |\nabla \chi| \\ &\leq C \frac{\epsilon^2}{h} |\chi|_{H^1(K)}, \end{aligned}$$

Now we may sum over all  $Y_\epsilon$  and  $Y'_\epsilon$  and note that all terms on the (4.11) and (4.16) are independent of  $\epsilon$  except the  $\epsilon$  itself. Thus,

$$(4.17) \quad \begin{aligned} \int_{z_l}^{z_m} (B_{ij} - \widetilde{B}_{ij}) (\chi - I_h \chi) \, ds &= \sum_{Y_\epsilon, Y'_\epsilon} \int_{Y_\epsilon} (B_{ij} - \widetilde{B}_{ij}) (\chi - I_h \chi) \, ds \\ &\leq C \frac{\epsilon}{h} |\chi|_{H^1(K)} \sum_{Y_\epsilon, Y'_\epsilon} \epsilon \\ &\leq C \epsilon |\chi|_{H^1(K)} \end{aligned}$$

The same procedure described above may be implemented for  $(z_m, z_r)$  so that summing up result from these two segments and applying inverse inequality to  $v_0^h$  give us

$$(4.18) \quad n_i \nabla_j v_0^h \int_e (B_{ij}(x/\epsilon) - \widetilde{B}_{ij}) (\chi - I_h \chi) \, ds \leq C \frac{\epsilon}{h} |v_0^h|_{H^1(K)} |\chi|_{H^1(K)}.$$

Then the right hand side of (4.3) in Lemma 4.1 finishes up the proof.  $\square$

**Lemma 4.3.** *Let  $e$  be an edge of triangle  $K$ , and  $\theta^h$  be as in (3.13). Then for every  $\chi \in X_h$  there exists constant  $C > 0$  independent of  $\epsilon$  and  $h$  such that*

$$(4.19) \quad \int_e A(x/\epsilon) \epsilon \nabla \theta^h \cdot \vec{n} (\chi - I_h \chi) \, ds \leq C \frac{\epsilon}{h} |v_\epsilon^h|_{H^1(K)} |\chi|_{H^1(K)}.$$

*Proof.* Using (3.13), Lemma 3.2, and the fact that  $\chi$  is linear on  $e$ , we have

$$\begin{aligned}
\int_e A(x/\epsilon) \epsilon \nabla \theta^h \cdot \vec{n} (\chi - I_h \chi) ds &\leq C \frac{\epsilon}{h} |\nabla v_0^h| \int_e |\chi - I_h \chi| ds \\
(4.20) \qquad \qquad \qquad &\leq C \frac{\epsilon}{h} |\nabla v_0^h| h \|\chi - I_h \chi\|_{L^\infty(e)} \\
&\leq C \frac{\epsilon}{h} |v_0^h|_{H^1(K)} |\nabla \chi| h \\
&\leq C \frac{\epsilon}{h} |v_0^h|_{H^1(K)} |\chi|_{H^1(K)},
\end{aligned}$$

where we have used inverse inequality for  $\nabla v_0^h$  and  $\nabla \chi$ . Then right hand side of (4.3) in Lemma 4.1 finishes up the proof.  $\square$

**Theorem 4.1.** *For  $v_\epsilon^h \in V_h$  we have*

$$(4.21) \qquad |D(v_\epsilon^h, \chi)| \leq C_d \frac{\epsilon}{h} |v_\epsilon^h|_{1,h} |\chi|_{H^1} \quad \forall \chi \in X_h.$$

*Proof.* Considering (4.7), we may break up the integral over  $\partial K$  into the sum of integral over the edges  $e$ . Then the estimate is obtained by straightforward application of Lemmas 4.2 and 4.3.  $\square$

**4.2. Inf-Sup conditions and error estimates.** We start by establishing the inf-sup condition of the finite element bilinear form. Similar proof has also been conducted in [21]. Moreover, in [21] the authors derived an  $L_2$  error estimate for the two-scale nonconforming Petrov-Galerkin finite element and demonstrated the smallness of the nonconforming error.

**Lemma 4.4.** *Assume that (4.2) holds. Then the finite element bilinear form (3.23) satisfies the inf-sup condition, i.e., for  $v_\epsilon^h \in V_h$  we have*

$$(4.22) \qquad \sup_{\chi \in X_h} \frac{a_{FE}(v_\epsilon^h, \chi)}{\|\chi\|_{H^1}} \geq C_{fe} \|v_\epsilon^h\|_{1,h}$$

for some constant  $C_{fe} > 0$  independent of  $\epsilon, h$ .

*Proof.* Let us define a  $2 \times 2$  matrix  $M(x/\epsilon)$  whose entries are defined as

$$(4.23) \qquad M_{ij} = B_{ij} + \epsilon A_{ik} \nabla_k \eta_j,$$

where  $B_{ij}, \nabla_k$  and  $\eta_j$  are as in section 3.1. By using the expansion (3.14) and noting that  $v_0^h$  is piecewise linear, we may write (3.24) as

$$(4.24) \qquad a_{FE}(v_\epsilon^h, \chi) = \sum_{K \in T_h} (M(x/\epsilon) \nabla v_0^h, \nabla \chi)_K.$$

Now by Lemma 3.2 we may use the assumption (4.2) to the term  $M_{ij} = B_{ij} + \epsilon A_{ik} \nabla_k \eta_j$ , and thus by taking  $\chi = v_0^h$  we have

$$(4.25) \qquad \sup_{\chi \in X_h} \frac{a_{FE}(v_\epsilon^h, \chi)}{\|\chi\|_{H^1}} \geq C \frac{|v_0^h|_{1,h}^2}{\|v_0^h\|_{1,h}}.$$

Left hand side of (4.3) in Lemma 4.1 and the Poincaré-Friedrichs inequality finish up the proof.  $\square$

This inf-sup condition guarantees that there exists a unique solution to our two-scale finite element problem. Now we may establish a variation of Céa's Lemma written in the theorem below.

**Theorem 4.2.** *Let  $u_\epsilon$  and  $\tilde{u}_\epsilon^h$  be the solutions of (2.1) and (3.22), respectively. Then*

$$(4.26) \quad \|u_\epsilon - \tilde{u}_\epsilon^h\|_{1,h} \leq (1 + C_{fe}) \inf_{v_\epsilon^h \in V_h} \|u_\epsilon - v_\epsilon^h\|_{1,h}.$$

*Proof.* Let  $v_\epsilon^h \in V_h$  and  $\chi \in X_h$ . We have  $a_{FE}(\tilde{u}_\epsilon^h - v_\epsilon^h, \chi) = a_{FE}(u_\epsilon - v_\epsilon^h, \chi) + a_{FE}(\tilde{u}_\epsilon^h, \chi) - (f, \chi)$ , where the last two terms cancel each other. Using this fact and in view of Lemma 4.4 we have

$$(4.27) \quad \begin{aligned} \|\tilde{u}_\epsilon^h - v_\epsilon^h\|_{1,h} &\leq C_{fe} \sup_{\chi \in X_h} \frac{a_{FE}(u_\epsilon - v_\epsilon^h, \chi)}{\|\chi\|_{H^1}} \\ &\leq C_{fe} \|u_\epsilon - v_\epsilon^h\|_{1,h}. \end{aligned}$$

The result follows from the triangle inequality  $\|u_\epsilon - \tilde{u}_\epsilon^h\|_{1,h} \leq \|u_\epsilon - v_\epsilon^h\|_{1,h} + \|\tilde{u}_\epsilon^h - v_\epsilon^h\|_{1,h}$  and by taking the infimum over all elements of  $V_h$ .  $\square$

Next lemma is devoted to establishing the inf-sup condition of the two-scale finite volume element bilinear form. The proof uses a standard procedure for the finite volume element method perturbation argument.

**Lemma 4.5.** *For sufficiently small ratio  $\epsilon/h$  the finite volume element bilinear form (3.20) satisfies inf-sup condition, i.e., for  $v_\epsilon^h \in V_h$  there exists a constant  $C_{fv} > 0$  such that*

$$(4.28) \quad \sup_{\chi \in X_h} \frac{a_{FV}(v_\epsilon^h, I_h \chi)}{\|\chi\|_{H^1}} \geq C_{fv} \|v_\epsilon^h\|_{1,h}.$$

*Proof.* Using (3.26) we may write

$$(4.29) \quad a_{FV}(v_\epsilon^h, I_h \chi) = a_{FE}(v_\epsilon^h, \chi) - D(v_\epsilon^h, \chi)$$

By Lemma 4.4 and Theorem 4.1 we have

$$(4.30) \quad \sup_{\chi \in X_h} \frac{a_{FV}(v_\epsilon^h, I_h \chi)}{\|\chi\|_{H^1}} \geq \left( C_{fe} - C_d \frac{\epsilon}{h} \right) \|v_\epsilon^h\|_{1,h}.$$

Thus for sufficiently small  $\epsilon/h$  we have  $C_{fv} = C_{fe} - C_d \epsilon/h$  positive.  $\square$

Hence, as in the finite element case, we guarantee the existence and uniqueness of the two-scale finite volume element solution by this inf-sup condition. We note that the following lemma is a consequence of Lemma 4.5.

**Lemma 4.6.** *Let  $u_\epsilon^h \in V_h$  be the solution of (3.21) associated with (2.1). Then*

$$(4.31) \quad \|u_\epsilon^h\|_{1,h} \leq C \|f\|.$$

*Proof.* By Lemma 4.5 and (3.21) we have

$$(4.32) \quad C_{fv} \|u_\epsilon^h\|_{1,h} \leq \sup_{\chi \in X_h} \frac{(f, I_h \chi)}{\|\chi\|_{H^1}}.$$

Now using Cauchy-Schwarz inequality and (2.6) we have the result.  $\square$

Next we show that the difference between the two-scale finite volume element and two-scale finite element solutions is small.

**Lemma 4.7.** *Let  $u_\epsilon^h \in V_h$  be the solution of (3.21), and  $\tilde{u}_\epsilon^h \in V_h$  be the solution of (3.22), both associated with (2.1). Then we have*

$$(4.33) \quad \|\tilde{u}_\epsilon^h - u_\epsilon^h\|_{1,h} \leq \left( C_1 h + C_2 \frac{\epsilon}{h} \right) \|f\|.$$

*Proof.* First we introduce a bilinear form

$$(4.34) \quad d(f, \chi) = (f, \chi - I_h \chi) \quad \forall f \in L_2, \chi \in X_h.$$

This bilinear form has the following approximation property [2, Lemma 5.1]:

$$(4.35) \quad |d(f, \chi)| \leq C h \|f\| \|\chi\|_{H^1}.$$

Using (4.34) and (3.26), we may write

$$(4.36) \quad a_{FE}(\tilde{u}_\epsilon^h - u_\epsilon^h, \chi) = d(f, \chi) - D(u_\epsilon^h, \chi) \quad \forall \chi \in X_h.$$

The terms on the right hand side of this equation are estimated in (4.35) and Theorem 4.1. Dividing both sides by  $\|\chi\|_{H^1}$  and taking supremum over all  $\chi$  we have

$$(4.37) \quad \sup_{\chi \in X_h} \frac{a_{FE}(\tilde{u}_\epsilon^h - u_\epsilon^h, \chi)}{\|\chi\|_{H^1}} \leq \left( C_1 h \|f\| + C_d \frac{\epsilon}{h} \|u_\epsilon^h\|_{1,h} \right).$$

But Lemma 4.6 guarantees the boundedness of  $u_\epsilon^h$ , and thus by Lemma 4.5 we have the result.  $\square$

**Theorem 4.3.** *Let  $u_\epsilon$  and  $u_\epsilon^h$  be the solutions of (2.1) and (3.21), respectively. Then,*

$$(4.38) \quad \|u_\epsilon - u_\epsilon^h\|_{1,h} \leq \left( C_1 h + C_2 \frac{\epsilon}{h} \right) \|f\| + C_3 \inf_{v_\epsilon^h \in V_h} \|u_\epsilon - v_\epsilon^h\|_{1,h}.$$

*Proof.* Let  $\tilde{u}_\epsilon^h$  be the solution of (3.22). Using triangle inequality we have

$$(4.39) \quad \|u_\epsilon - u_\epsilon^h\|_{1,h} \leq \|u_\epsilon - \tilde{u}_\epsilon^h\|_{1,h} + \|\tilde{u}_\epsilon^h - u_\epsilon^h\|_{1,h}.$$

In view of Lemma 4.7 it suffices to prove the first part. Now let  $v_\epsilon^h \in V_h$ . By triangle inequality, Lemma 4.4 and orthogonality of  $a_{FE}(\cdot, \cdot)$  we have

$$\begin{aligned}
(4.40) \quad \|u_\epsilon - \tilde{u}_\epsilon^h\|_{1,h} &\leq \|u_\epsilon - v_\epsilon^h\|_{1,h} + \|\tilde{u}_\epsilon^h - v_\epsilon^h\|_{1,h} \\
&\leq \|u_\epsilon - v_\epsilon^h\|_{1,h} + \sup_{\chi \in X_h} \frac{a_{FE}(\tilde{u}_\epsilon^h - v_\epsilon^h, \chi)}{\|\chi\|_{H^1}} \\
&= \|u_\epsilon - v_\epsilon^h\|_{1,h} + \sup_{\chi \in X_h} \frac{a_{FE}(u_\epsilon - v_\epsilon^h, \chi)}{\|\chi\|_{H^1}} \\
&\leq C \|u_\epsilon - v_\epsilon^h\|_{1,h}.
\end{aligned}$$

Since  $v_\epsilon^h \in V_h$  is arbitrary, we may take the infimum over all elements of  $V_h$ , and the desired estimate follows.  $\square$

**Lemma 4.8.** *Let  $u_\epsilon$  be the solution of (2.1). Choose  $v_\epsilon^h$  an element of  $V_h$  such that for each triangle  $K \in T_h$   $v_0^h(z) = u_0(z)$ ,  $z \in Z_h(K)$ , i.e., the homogenized part of  $v_\epsilon^h$  coincides with the homogenized part of  $u_\epsilon$  on the vertices of the triangles. Then there exists a constant  $C > 0$  independent of  $\epsilon$  and  $h$  such that*

$$(4.41) \quad \|u_\epsilon - v_\epsilon^h\|_{1,h} \leq C \left( h |u_0|_{H^2} + \frac{\epsilon}{h} |u_0|_{H^1} + \sqrt{\epsilon} \right).$$

*Proof.* By definition of the norm, it suffices to establish the estimate over a triangle  $K$ . Using the expansion (3.2) and (3.14), we have

$$(4.42) \quad u_\epsilon - v_\epsilon^h = (u_0 - v_0^h) + \epsilon N_k \nabla_k (u_0 - v_0^h) + \epsilon \theta_u + \epsilon \theta^h.$$

It has been well known that since  $v_0^h$  is linear on  $K$ , the following estimate holds:

$$(4.43) \quad |u_0 - v_0^h|_{H^1(K)} \leq C h |u_0|_{H^2(K)}.$$

Now since  $A_{ij} \in W_p^1(Y)$ ,  $\epsilon \nabla N_k$  is locally bounded. Hence

$$(4.44) \quad \begin{aligned} |\epsilon N_k \nabla_k (u_0 - v_0^h)|_{H^1(K)} &\leq \max\{\epsilon \|\nabla N_1\|_{L^\infty(K)}, \epsilon \|\nabla N_2\|_{L^\infty(K)}\} |u_0 - v_0^h|_{H^1(K)} \\ &\leq C h |u_0|_{H^2(K)}. \end{aligned}$$

Next using (3.13) and applying Lemma 3.2, we have

$$(4.45) \quad \epsilon^2 |\theta^h|_{H^1(K)}^2 \leq \epsilon^2 \int_K |\nabla \eta_k|^2 |\nabla_k v_0^h|^2 dx \leq C \frac{\epsilon^2}{h^2} |v_0^h|_{H^1(K)}^2.$$

Moreover, it is clear that using triangle inequality, (4.43) we have

$$|v_0^h|_{H^1(K)} \leq C h |u_0|_{H^2(K)} + |u_0|_{H^1(K)}.$$

Finally, summing up over all triangles  $K \in T_h$  and using Lemma 3.1 to estimate  $\theta^u$ , we obtain the desired estimate.  $\square$

From Theorem 4.2, Theorem 4.3 Lemma 4.8 we immediately obtain the following:

**Corollary 4.1.** *Let  $u_\epsilon$  and  $\tilde{u}_\epsilon^h$  be the solutions of (2.1) and (3.22), respectively. Then there exists a constant  $C > 0$  independent of  $\epsilon$  and  $h$  such that*

$$(4.46) \quad \|u_\epsilon - \tilde{u}_\epsilon^h\|_{1,h} \leq C_1 h + C_2 \frac{\epsilon}{h} + C_3 \sqrt{\epsilon}.$$

**Corollary 4.2.** *Let  $u_\epsilon$  and  $u_\epsilon^h$  be the solutions of (2.1) and (3.21), respectively. Then there exists a constant  $C > 0$  independent of  $\epsilon$  and  $h$  such that*

$$(4.47) \quad \|u_\epsilon - u_\epsilon^h\|_{1,h} \leq C_1 h + C_2 \frac{\epsilon}{h} + C_3 \sqrt{\epsilon}.$$

Therefore, both finite element and finite volume element for two-scale method have the same asymptotic convergence rates.

## 5. NUMERICAL EXAMPLES

In this section we present numerical experiments to assess the performance of the two-scale finite volume element method. A convergence test of the method is reported which is followed by an application to flow in porous media. In all of these computations, we have used finely resolved numerical solutions obtained using finite volume method as reference solutions. This is because it is extremely hard to come up with a boundary value problem which has an exact solution. All the examples below use a unit square domain,  $\Omega = (0, 1) \times (0, 1)$ .

**5.1. Convergence Test.** For the convergence test, the methods are tested by solving (2.1) with the periodic coefficient cf. [15]

$$A(x/\epsilon) = \frac{2 + 1.8 \sin(2\pi x_1/\epsilon)}{2 + 1.8 \cos(2\pi x_2/\epsilon)} + \frac{2 + \sin(2\pi x_2/\epsilon)}{2 + 1.8 \cos(2\pi x_1/\epsilon)}$$

and

$$f = -1.$$

The computation is implemented on a uniform rectangular mesh. Here  $N$  is the number of coarse elements in each direction and  $n$  the number in each direction of sub-elements in a coarse element.

In the following, the error is denoted by  $e = u_\epsilon - u_\epsilon^h$ , TS-FV denotes the two-scale finite volume element method using conforming basis functions and TS-FV-O denotes the two-scale finite volume element method with oversampling strategy. To investigate the interaction between the components of error written in Corrolary 4.2, we show three sets of scenario whose results are listed in three different tables. The first scenario deals with a constant  $\epsilon$  while varying the number of coarse elements  $N$ . For this, the reference solution is resolved on a mesh with 2048 elements in each direction. On the other hand, the second scenario deals with a constant ratio  $\epsilon/h$  and a constant number of sub-elements  $n$ . Thus once an  $\epsilon$  is given, the number of coarse element may be obtained from the specified ratio. Consequently, for each case in this second scenario, the number of total elements used to resolve the reference solution would be different. Finally, the third scenario uses a constant number of coarse elements  $N$ , while varying the  $\epsilon$  (and consequently varying  $n$  also).



TABLE 1. Comparison of  $H^1$  seminorm of solution error for  $\epsilon = 0.005$ .

$N$	$n$	TS-FV	TS-FV-O	
		$ e _1$	$ e _1$	Rate
32	64	$2.142806 \times 10^{-2}$	$8.188009 \times 10^{-3}$	-
64	32	$2.926952 \times 10^{-2}$	$4.114026 \times 10^{-3}$	0.993
128	16	$4.473100 \times 10^{-2}$	$2.288907 \times 10^{-3}$	0.846
256	8	$5.951678 \times 10^{-2}$	$1.911220 \times 10^{-3}$	0.260

TABLE 2. Comparison of  $H^1$  seminorm of error for  $\epsilon/h = 0.64$  and  $n = 16$ .

$N$	$\epsilon$	TS-FV	TS-FV-O	
		$ e _1$	$ e _1$	Rate
16	0.040	$5.031755 \times 10^{-2}$	$2.419640 \times 10^{-2}$	-
32	0.020	$4.510508 \times 10^{-2}$	$8.427971 \times 10^{-3}$	1.522
64	0.010	$4.475054 \times 10^{-2}$	$4.388929 \times 10^{-3}$	0.941
128	0.005	$4.473100 \times 10^{-2}$	$2.288907 \times 10^{-3}$	0.939

All results pertaining to the error of the solution in  $H^1$  norm are listed in Tables 1, 2, and 3. In general we see a significant improvement using the oversampling strategy (TS-FV-O). Table 1 shows comparison of the  $H_1$  norm of the error of the approximation taken against the number of elements  $N$  and  $n$  with a constant  $\epsilon$  equal to 0.005. Obviously, TS-FV gives the worst results for fixed  $N \times n$  with  $n$  decreasing since we have introduced more intercourse finite element boundaries, which in turn generate some errors. It may be seen from Table 1, that when preserving the  $\epsilon$ , and letting the  $h$  decreases, the convergence in TS-FV-O (also in TS-FV) deteriorates when  $\epsilon/h \approx 1$ . It should be pointed out that for cases around this regime, Corrolary 4.2 might not be true anymore. In Table 2 we present the corresponding error in the case of the ratio  $\epsilon/h = 0.64$  and  $n = 16$ . From Table 2 we see that the first order convergence for TS-FV-O is relatively maintained irrespective of the value of  $h$ . This phenomenon gives a hint that the  $O(\epsilon)$  constant ( $C_3$ ) in Corrolary 4.2 is smaller than the  $O(h)$  constant ( $C_1$ ). Finally Table 3 gives the comparison for a constant  $N = 32$  and varying  $\epsilon$ . The table indicates that the TS-FV-O errors do not change significantly compared to TS-FV errors, which suggests that the  $O(\epsilon/h)$  is more dominant in TS-FV than in TS-FV-O. This fact shows that the oversampling strategy has reduced the resonance error inherent in the original two-scale method. Similar comparisons for  $L_2$  norm errors are presented in Tables 4, 5, and 6. It is apparent that they exhibit similar behaviors as in  $H_1$  norm. This finding is consistent with the investigation conducted by the authors of [21].

**5.2. Application to Flow in Porous Media.** In this subsection we present an application of the two-scale finite volume element method to a flow in porous medium. The problem considered is typical representation of a cross section of a subsurface. In this case, (2.1) governs a pressure distribution over the domain. As before we set our domain  $\Omega = (0, 1) \times (0, 1)$ , with a given pressure on the left and right boundaries, i.e.,  $u(x_1 = 0, x_2) = 1$ , and

TABLE 3. Comparison of  $H^1$  seminorm of error for  $N = 32$ .

$\epsilon$	$n$	TS-FV	TS-FV-O
		$ e _1$	$ e _1$
0.020	16	$4.510508 \times 10^{-2}$	$8.427971 \times 10^{-3}$
0.010	32	$2.975713 \times 10^{-2}$	$8.195283 \times 10^{-3}$
0.005	64	$2.142806 \times 10^{-2}$	$8.188009 \times 10^{-3}$

TABLE 4. Comparison of  $L_2$  norm of solution error for  $\epsilon = 0.005$ .

$N$	$n$	TS-FV	TS-FV-O	
		$\ e\ $	$\ e\ $	Rate
32	64	$8.735775 \times 10^{-5}$	$1.938853 \times 10^{-5}$	-
64	32	$1.720292 \times 10^{-4}$	$4.812917 \times 10^{-6}$	2.010
128	16	$2.941193 \times 10^{-4}$	$2.336342 \times 10^{-6}$	1.043
256	8	$3.683877 \times 10^{-4}$	$6.251241 \times 10^{-7}$	1.902

TABLE 5. Comparison of  $L_2$  norm of error for  $\epsilon/h = 0.64$ , and  $n = 16$ .

$N$	$\epsilon$	TS-FV	TS-FV-O	
		$\ e\ $	$\ e\ $	Rate
16	0.040	$3.898167 \times 10^{-4}$	$8.649052 \times 10^{-5}$	-
32	0.020	$3.172062 \times 10^{-4}$	$2.146057 \times 10^{-5}$	2.011
64	0.010	$2.986045 \times 10^{-4}$	$5.077901 \times 10^{-6}$	2.079
128	0.005	$2.941193 \times 10^{-4}$	$2.336342 \times 10^{-6}$	1.120

TABLE 6. Comparison of  $L_2$  norm of error for  $N = 32$ .

$\epsilon$	$n$	TS-FV	TS-FV-O
		$\ e\ $	$\ e\ $
0.020	16	$3.172062 \times 10^{-4}$	$2.146057 \times 10^{-5}$
0.010	32	$2.086535 \times 10^{-4}$	$1.886330 \times 10^{-5}$
0.005	64	$8.735775 \times 10^{-5}$	$1.938853 \times 10^{-5}$

$u(x_1 = 1, x_2) = 0$  while the top and bottom boundaries are closed to flow, i.e.  $u_{x_2}(x_1, x_2 = 0) = u_{x_2}(x_1, x_2 = 1) = 0$ . For this example, the finely resolved model uses  $1024 \times 1024$  elements.

Moreover, the matrix  $A$  is set to be a diagonal matrix with  $A_{ii}(x) = k(x)$ , which is called the absolute permeability. Instead of using a periodic functions, we use  $k(x)$  as a set of randomly generated numbers realized in  $1025 \times 1025$  grid points, given its correlation structures ( $l_{x_1}$ , and  $l_{x_2}$ ), covariance model and overall variance quantified via  $\sigma^2$  which is the variance of  $\log k$ . We consider a GSLIB model developed in [6].

In the examples below, we concentrate on the anisotropic case, where in practical application is the most difficult to upscale. We have used  $l_{x_1} = 0.4$  and  $l_{x_2} = 0.01$  with exponential

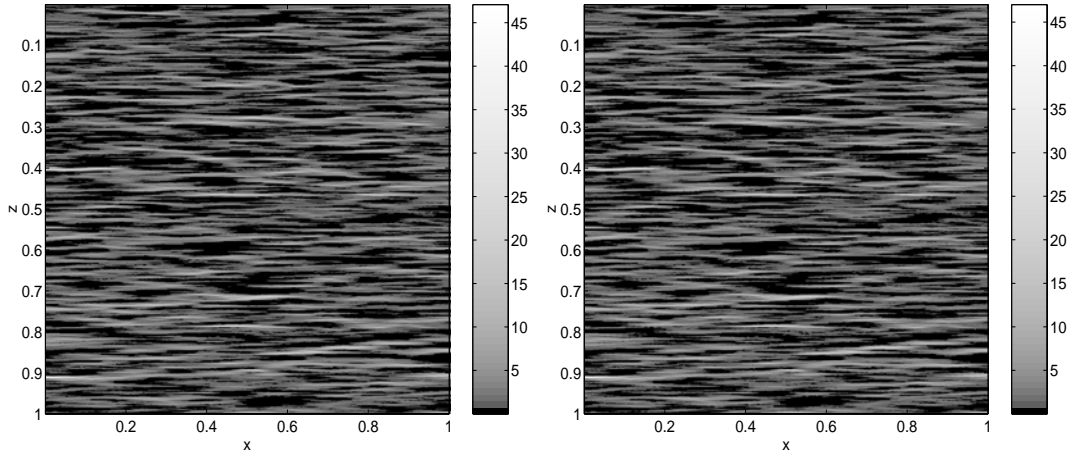


FIGURE 4. Comparison of horizontal velocity for anisotropic absolute permeability with  $\sigma = 1.5$ : (left) finely resolved model with  $1024 \times 1024$  elements, (right) two-scale FVE with  $64 \times 64$  coarse elements

TABLE 7. Results for anisotropic case,  $l_{x_1} = 0.40$ ,  $l_{x_2} = 0.01$ ,  $\sigma = 1.0$ .

$N$	$n$	$e$	$e_r$ (%)	$e_{x_1}$	$e_{x_1,r}$ (%)
32	32	$2.260724 \times 10^{-4}$	0.039	$3.532075 \times 10^{-2}$	1.97
64	16	$1.198503 \times 10^{-4}$	0.021	$2.741758 \times 10^{-2}$	1.53
128	8	$8.155836 \times 10^{-5}$	0.014	$2.305173 \times 10^{-2}$	1.28
256	4	$5.907592 \times 10^{-5}$	0.010	$1.928818 \times 10^{-2}$	1.07

TABLE 8. Results for anisotropic case,  $l_{x_1} = 0.40$ ,  $l_{x_2} = 0.01$ ,  $\sigma = 1.5$ .

$N$	$n$	$e$	$e_r$ (%)	$e_{x_1}$	$e_{x_1,r}$ (%)
32	32	$8.140234 \times 10^{-4}$	0.141	$1.197157 \times 10^{-1}$	3.80
64	16	$4.406654 \times 10^{-4}$	0.076	$8.694687 \times 10^{-2}$	2.76
128	8	$3.198741 \times 10^{-4}$	0.055	$6.950237 \times 10^{-2}$	2.20
256	4	$2.022701 \times 10^{-4}$	0.035	$5.643796 \times 10^{-2}$	1.79

covariance model, and  $\sigma = 1.0$ . Table 7 presents the pressure error  $e = \|u - u^h\|$  and the horizontal velocity error  $e_{x_1} = \|k(u_{x_1} - u_{x_1}^h)\|$ , and their corresponding relative errors,  $e_r = e/\|u\|$ , and  $e_{x_1,r} = e_{x_1}/\|ku_{x_1}\|$ . On the second example shown in Table 8, we use the same correlation lengths and structures, and  $\sigma = 1.5$ . In all examples, we see that as  $h$  decreases, the errors decrease as well. Comparison of the visualized horizontal velocities are shown in Figure 4.

## 6. SUMMARY

In this paper we have proposed a two-scale finite volume element method for solving a second order elliptic problem with fluctuating/heterogeneous coefficients. The method has the advantages of capturing the small scale effects on the large one, and numerically conservative on the coarse mesh. The analysis presented reveals that in the case of periodic coefficients, the method converges to the homogenized solution as  $\epsilon \rightarrow 0$ . Although the analysis of the method was performed for periodic structures, the method itself is not limited only to this case. We have employed the two-scale finite volume element method for several applications such as upscaling for multiphase flow problem and nonlinear convective and parabolic equations [14].

## ACKNOWLEDGMENT

The author wishes to thank Dr. Raytcho Lazarov and Dr. Yalchin Efendiev for introducing the problem and their guidance in the development and analysis of the method. This work was partially supported by the NSF Grant EIA-0218229.

## REFERENCES

- [1] T. Arbogast and S. L. Bryant. Numerical subgrid upscaling for waterflood simulations. TICAM Report 01-23, <http://www.ticam.utexas.edu/reports/2001/index.html>.
- [2] P. Chatzipantelidis. Finite volume methods for elliptic PDE's: a new approach. *M2AN Math. Model. Numer. Anal.*, 36(2):307–324, 2002.
- [3] P. Chatzipantelidis, R. Lazarov, and V. Thomée. Error estimates for the finite volume element method for parabolic equations in convex polygonal domains. *ISC Technical Report Series*, 3, 2003.
- [4] S. Chou and Q. Li. Error estimates in  $L^2$ ,  $H^1$  and  $L^\infty$  in covolume methods for elliptic and parabolic problems: a unified approach. *Math. Comp.*, 69(229):103–120, 2000.
- [5] M. A. Christie. Upscaling for reservoir simulation. *J. Pet. Tech.*, pages 1004–1010, 1996.
- [6] C. V. Deutsch and A. G. Journel. *GSLIB: Geostatistical software library and user's guide, 2nd edition*. Oxford University Press, New York, 1998.
- [7] L. J. Durlofsky. Numerical calculation of equivalent grid block permeability tensors for heterogeneous porous media. *Water Resour. Res.*, 27:699–708, 1991.
- [8] L. J. Durlofsky. Representation of grid block permeability in coarse scale models of randomly heterogeneous porous-media. *Water Resour. Res.*, 28:1791–1800, 1992.
- [9] W. E and B. Engquist. The heterogeneous multi-scale methods. *Comm. Math. Sci.*, 1(1), 2003.
- [10] Y. R. Efendiev, T. Y. Hou, and X. H. Wu. Convergence of a nonconforming multiscale finite element method. *SIAM J. Num. Anal.*, 37:888–910, 2000.
- [11] R. E. Ewing. Upscaling of biological processes and multiphase flow in porous media. In *Fluid flow and transport in porous media: mathematical and numerical treatment (South Hadley, MA, 2001)*, volume 295 of *Contemp. Math.*, pages 195–215. Amer. Math. Soc., Providence, RI, 2002.
- [12] R. E. Ewing, T. Lin, and Y. Lin. On the accuracy of the finite volume element method based on piecewise linear polynomials. *SIAM J. Numer. Anal.*, 39(6):1865–1888 (electronic), 2002.
- [13] R. Eymard, T. Gallouët, and R. Herbin. Finite volume methods. In *Handbook of numerical analysis, Vol. VII*, Handb. Numer. Anal., VII, pages 713–1020. North-Holland, Amsterdam, 2000.
- [14] V. Ginting, R. Ewing, Y. Efendiev, and R. Lazarov. Upscaled modeling in multiphase flow applications. submitted to *Computational and Applied Mathematics*.
- [15] T. Y. Hou and X. H. Wu. A multiscale finite element method for elliptic problems in composite materials and porous media. *Journal of Computational Physics*, 134:169–189, 1997.

- [16] T. Y. Hou, X. H. Wu, and Z. Cai. Convergence of a multiscale finite element method for elliptic problems with rapidly oscillating coefficients. *Math. Comp.*, 68(227):913–943, 1999.
- [17] P. Jenny, S.H. Lee, and H.A. Tchelepi. Multi-scale finite-volume method for elliptic problems in sub-surface flow simulation. *Journal of Computational Physics*, 187:47–67, 2003.
- [18] V. V. Jikov, S. M. Kozlov, and O. A. Oleinik. *Homogenization of differential operators and integral functionals*. Springer-Verlag, New York, 1994.
- [19] R. Li, Z. Chen, and W. Wu. *Generalized difference methods for differential equations*, volume 226 of *Monographs and Textbooks in Pure and Applied Mathematics*. Marcel Dekker Inc., New York, 2000. Numerical analysis of finite volume methods.
- [20] X. H. Wen and J. J. Gomez-Hernandez. Upscaling hydraulic conductivities in heterogeneous media: an overview. *Journal of Hydrology*, 183:ix–xxxii, 1996.
- [21] Y. Zhang, T. Y. Hou, and X. H. Wu. Convergence of a nonconforming multiscale finite element method. *Preprint*, 1998.

DEPARTMENT OF MATHEMATICS, TEXAS A & M UNIVERSITY,  
COLLEGE STATION, TX 77843-3404  
*E-mail address:* `ginting@math.tamu.edu`